ARMY RESEARCH LABORATORY

Characterization of High Temperature Polymer Thin Films for Power Conditioning Capacitors

by Janet Ho and Richard Jow

ARL-TR-4880 **July 2009**

NOTICES

Disclaimers

The findings in this report are not to be construed as an official Department of the Army position unless so designated by other authorized documents.

Citation of manufacturer's or trade names does not constitute an official endorsement or approval of the use thereof.

Destroy this report when it is no longer needed. Do not return it to the originator.

Army Research Laboratory
Adelphi, MD 20783-1197

ARL-TR-4880 **July 2009**

Characterization of High Temperature Polymer Thin Films for Power Conditioning Capacitors

Janet Ho and Richard Jow
Sensors and Electron Devices Directorate, ARL

REPORT DOCUMENTATION PAGE

Form Approved
OMB No. 0704-0188

1. REPORT DATE *(DD-MM-YYYY)*	2. REPORT TYPE	3. DATES COVERED (From - To)
July 2009	Final	

4. TITLE AND SUBTITLE
Characterization of High Temperature Polymer Thin Films for Power Conditioning Capacitors

5a. CONTRACT NUMBER

5b. GRANT NUMBER

5c. PROGRAM ELEMENT NUMBER

6. AUTHOR(S)
Janet Ho and Richard Jow

5d. PROJECT NUMBER

5e. TASK NUMBER

5f. WORK UNIT NUMBER

7. PERFORMING ORGANIZATION NAME(S) AND ADDRESS(ES)
U.S. Army Research Laboratory
ATTN: RDRL-SED-C
2800 Powder Mill Road
Adelphi, MD 20783-1197

8. PERFORMING ORGANIZATION REPORT NUMBER
ARL-TR-4880

9. SPONSORING/MONITORING AGENCY NAME(S) AND ADDRESS(ES)

10. SPONSOR/MONITOR'S ACRONYM(S)

11. SPONSOR/MONITOR'S REPORT NUMBER(S)

12. DISTRIBUTION/AVAILABILITY STATEMENT
Approved for public release; distribution unlimited.

13. SUPPLEMENTARY NOTES

14. ABSTRACT
Capacitor dielectrics that can operate above 150 °C are needed for power electronics in military propulsion and weapons systems. This report characterized and compares two high temperature polymer film capacitor candidates, poly(ether imide) (PEI) and poly(ether ether ketone) (PEEK), with poly(phenylene sulfide) (PPS) and biaxially oriented polypropylene (BOPP), which offer limited performance at high temperature. Breakdown strength at room temperature was about 320 MV/m for PEEK, 500 MV/m for PPS and PEI, and 720 MV/m for BOPP. At 150 °C, breakdown strength for PEI decreased about 16% and about 13% for PEEK, while PPS remained unchanged. BOPP's maximum test temperature was 100 °C, at which breakdown strength decreased by about 11%. Dielectric loss measurements suggest PPS has greater electrical conductivity at 200 °C than PEEK or PEI, and PEI has a lower loss than PEEK at temperatures above 150 °C and frequencies higher than 1 kHz. The low E-field conductivity for PPS was 6.90×10^{-14} S/m at 165 °C and 1.72×10^{-11} S/m at 200 °C; the manufacturer listed room temperature conductivity as 2×10^{-16} S/m. The effect of conductivity on the temperature rise of the capacitors was analyzed. More measurements are needed to determine the conductivity of PEEK and PEI. Based on the measured data for breakdown strength and dielectric properties, PEI appears to be the better candidate.

15. SUBJECT TERMS
High temperature, polymer films caps, power electronics

16. SECURITY CLASSIFICATION OF:			17. LIMITATION OF ABSTRACT	18. NUMBER OF PAGES	19a. NAME OF RESPONSIBLE PERSON
a. REPORT	b. ABSTRACT	c. THIS PAGE			Janet Ho
Unclassified	Unclassified	Unclassified	UU	28	19b. TELEPHONE NUMBER (*Include area code*) (301) 394-0051

Standard Form 298 (Rev. 8/98)
Prescribed by ANSI Std. Z39.18

Contents

List of Figures

List of Tables

Acknowledgments

We would like to thank the following film suppliers: Patricia Irwin of GE Global Research Center for poly(ether imide) (PEI), Paul Knollmeyer of Toray for poly(phenylene sulfide) (PPS), and Phil Fox under contract with the Army Capacitor ManTech Program for poly(ether ether ketone) (PEEK).

INTENTIONALLY LEFT BLANK.

1. Introduction

The demand for high temperature capacitor dielectrics in power electronics is increasing with the electrification of military propulsion and weapons systems. Moving towards wide bandgap semiconductors (e.g., silicon carbide [SiC]) will enable operation at temperatures above 150 °C, which eases thermal management. However, such systems cannot be designed efficiently unless capacitors are available that can operate at similarly high temperatures.

Metallized polymer film capacitors have the advantage of self-healing, which allows graceful failure (*1*), i.e., a gradual loss in capacitance, rather than catastrophic failure as in ceramic capacitors. As a result, the capacitor dielectric can be operated at an electric field near the dielectric breakdown strength, thus achieving higher energy density. The state of the art in capacitor films is biaxially oriented polypropylene (BOPP), which has a low loss ($\tan \delta \sim 1 \times 10^{-4}$) that is independent of frequency and a high dielectric strength (~700 MV/m). The disadvantage of BOPP is that at temperatures above 85 °C, the operating voltage must be derated, and the maximum operating temperature is limited to about 105 °C.

Other commercially available polymer film capacitors that can be operated over a wider temperature range include poly(ethylene terephthalate) (PET), poly(ethylene napthalate) (PEN), polycarbonate (PC), poly(phenylene sulfide) (PPS), and Teflon. However, only PPS and Teflon can be operated at 150 °C and up to 200 °C, respectively. PPS has a poor self-healing capability, and Teflon has a low breakdown strength. As a result, neither of the presently available high temperature capacitor dielectrics is likely to satisfy military requirements for reliability and operating temperature on power electronics.

Poly(ether ether ketone) (PEEK) and poly(ether imide) (PEI) are two commercially available thin films (<12 μm) that are candidates for high temperature applications, as their glass transition temperature is above 150 °C. This report characterizes these two polymer films over a wide range of temperatures and compares them to BOPP and PPS.

2. Experimental

2.1 Materials

The materials studied were 12 μm (nominal) PEEK from Victrex, 6 μm (nominal) PEI from General Electric, 9 μm (nominal) PPS from Toray, and 7 μm (nominal) BOPP from Kopafilm. PPS and BOPP were used as benchmarks. All samples were used as is.

2.2 Thermal Analysis

The glass transition temperature (T_g) and crystalline melting temperature (T_m) of the samples were measured at a heating rate of 10 °C/min in nitrogen using differential scanning calorimetry (DSC) (Model DSC 2920, TA Instruments), as shown in figure 1.

Figure 1. Differential scanning calorimeter by TA Instruments.

2.3 Breakdown Strength Measurement

Figure 2 shows the configuration for breakdown strength measurement. Metallized films with metallization facing the test sample were used as electrodes. To define the active area for the breakdown measurement, a 100-μm thick polyimide mask with a window was placed in between the top electrode and the film under test. The active area was 2 cm^2. When voltage is applied, the layers are drawn together by electrostatic force, creating smooth interfaces without trapped air bubbles. Near the typical breakdown field of 700 MV/m, the pressure generated by the electrostatic force is ~5 MPa.

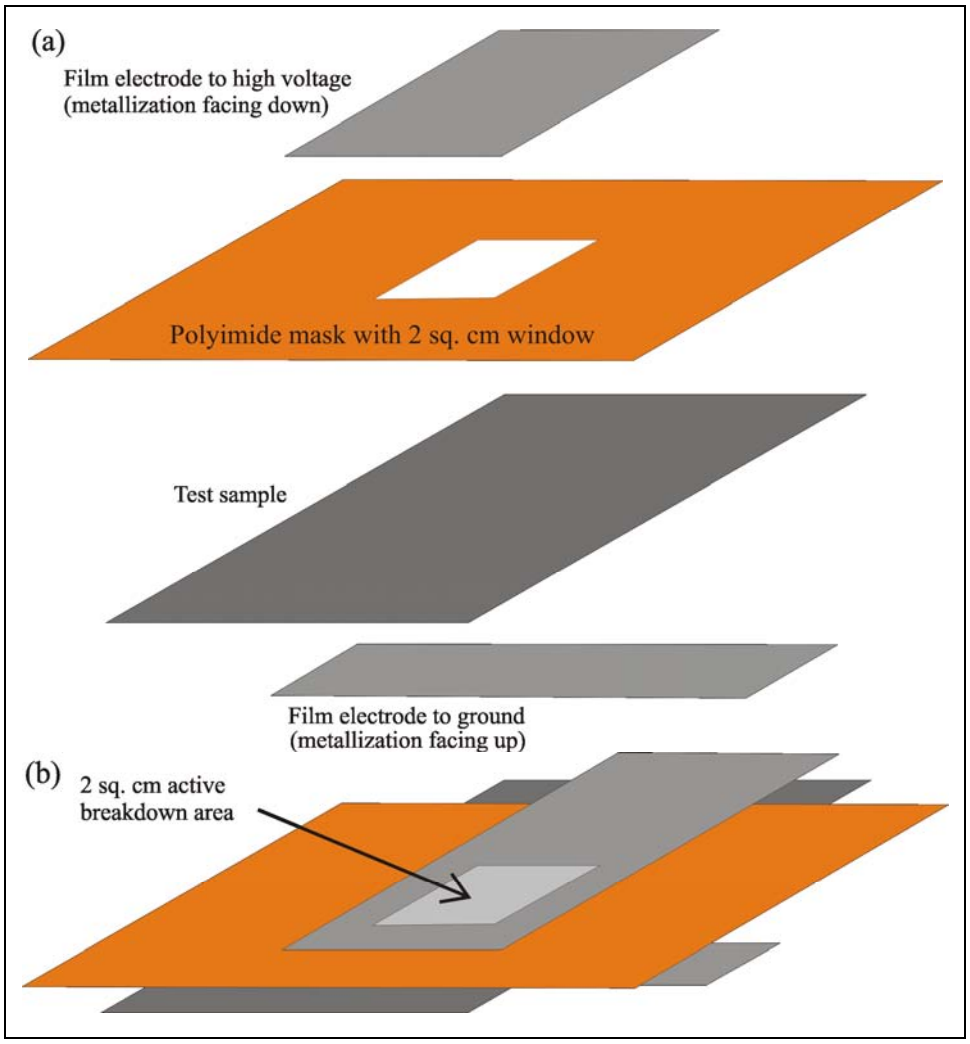

Figure 2. Schematic of the breakdown strength measurement setup, showing (a) the four individual layers separated and (b) the configuration during measurement.

Breakdown strength measurements were performed using a linear voltage ramp of 300 V/s, which is generated by a resistor capacitor (RC) circuit used to control the high voltage power supply as shown in figure 3. When the first breakdown event occurs, the power supply is shut off through an interlock input by a silicon controlled rectifier (SCR) circuit, which uses the breakdown-induced ground-rise voltage capacitively coupled to the gate of an SCR. The breakdown voltage of the sample is read from a peak-holding voltmeter, the internal impedance of which is employed as the "bottom" of a resistive divider. A new set of film electrodes was used for each measurement. Using metallized film instead of metal blocks as electrodes eliminates the need for polishing the electrode surface to remove the pits/craters caused by the breakdown events, which, if not removed, may reduce the breakdown strength of the samples due to local electric field enhancement. The sample thickness required for calculating the breakdown field was determined as the average of several measurements near the breakdown site. Figure 4 shows the thickness gauge (Model LE1000-2, MeasureItAll) employed to measure the thickness. It has a guaranteed absolute accuracy of 0.2 μm.

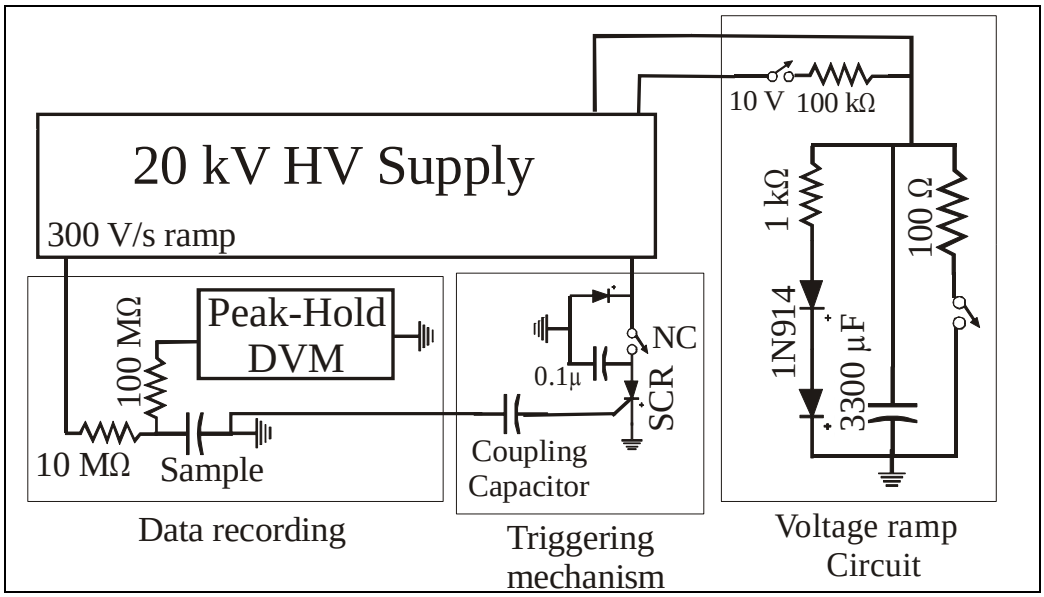

Figure 3. The circuit block diagram for breakdown strength measurement.

Figure 4. Thickness gauge by MeasureItAll.

Breakdown strength measurements at elevated temperature were conducted in an enclosed heated stage with an additional heater above the sample to reduce heat loss, as shown in figure 5. The sample setup was equilibrated at the test temperature for five minutes prior to measurements. A thermocouple was placed on the heated stage away from the active area to monitor the temperature.

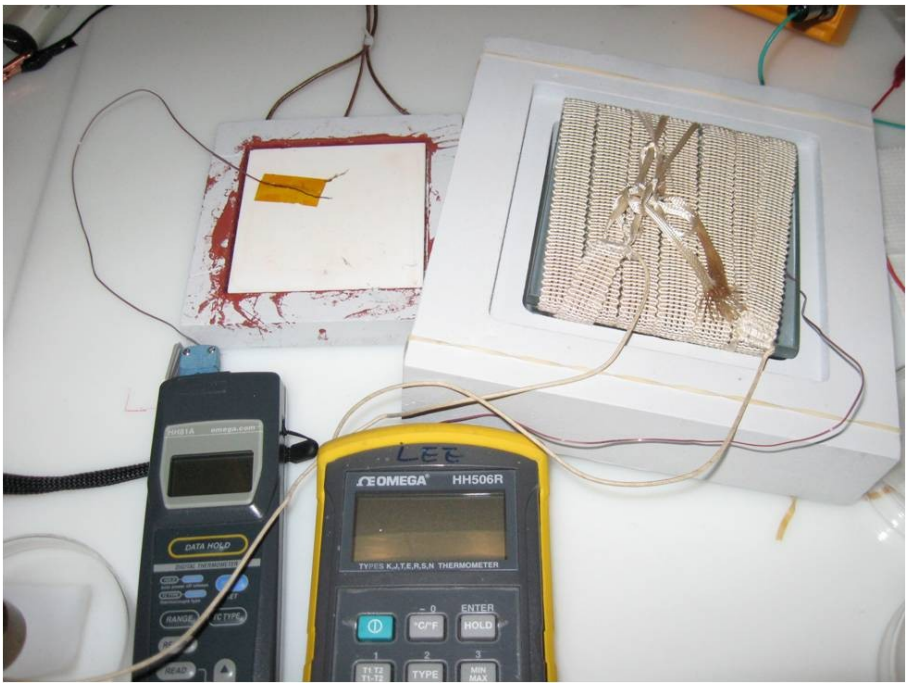

Figure 5. Enclosed heated stage for breakdown strength measurements at elevated temperature.

2.4 Dielectric Spectroscopy

Dielectric constant and dissipation factor (loss tangent) as a function of frequency at various temperatures were measured using a broadband dielectric spectrometer by Novocontrol, which is shown in figure 6. A 2-cm diameter of gold electrode with a surface resistivity of less than 10 Ω/square was sputtered on the samples.

Figure 6. Broadband dielectric spectrometer by Novocontrol.

3. Statistical Analysis

The Weibull distribution, which is based on the weak-link theory, is commonly employed for characterizing dielectric breakdown data (*2*), although other statistical distributions such as smallest extreme-value distribution or log-normal distribution are sometimes used. The Weibull distribution function (*3*), *F(x)*, is given as

$$\left\{ \begin{array}{ll} F(x) = 1 - \exp\left[-\left(\frac{x-c}{\eta}\right)^{\beta} \right] & \text{for } x \geq c \\ F(x) = 0 & \text{for } x < c \end{array} \right\}, \qquad (1)$$

where x is the electric field; η is the Weibull characteristic breakdown field, i.e., the breakdown field at 63.2% probability of breakdown ($x=\eta+c$, $F(x)=0.632$); β is the Weibull slope parameter, which is a measure of dispersion in the data; and c is the threshold field below which no breakdown will occur. The 2-parameter Weibull distribution is obtained when $c=0$ and is employed in the present analysis.

4. Results

4.1 Thermal Properties

The DSC thermograms for PEI, PEEK, PPS, and BOPP are shown in figure 7. PEI is an amorphous polymer and therefore does not show a crystalline melting peak as do the other three polymers, which are semi-crystalline. Table 1 summarizes the glass-transition temperature, the melting temperature, and the percent crystallinity of the samples. The values for heat of fusion of PEEK, PPS, and BOPP at 100% crystallinity used for calculating the percent crystallinity of the samples are taken from references 4–6, respectively.

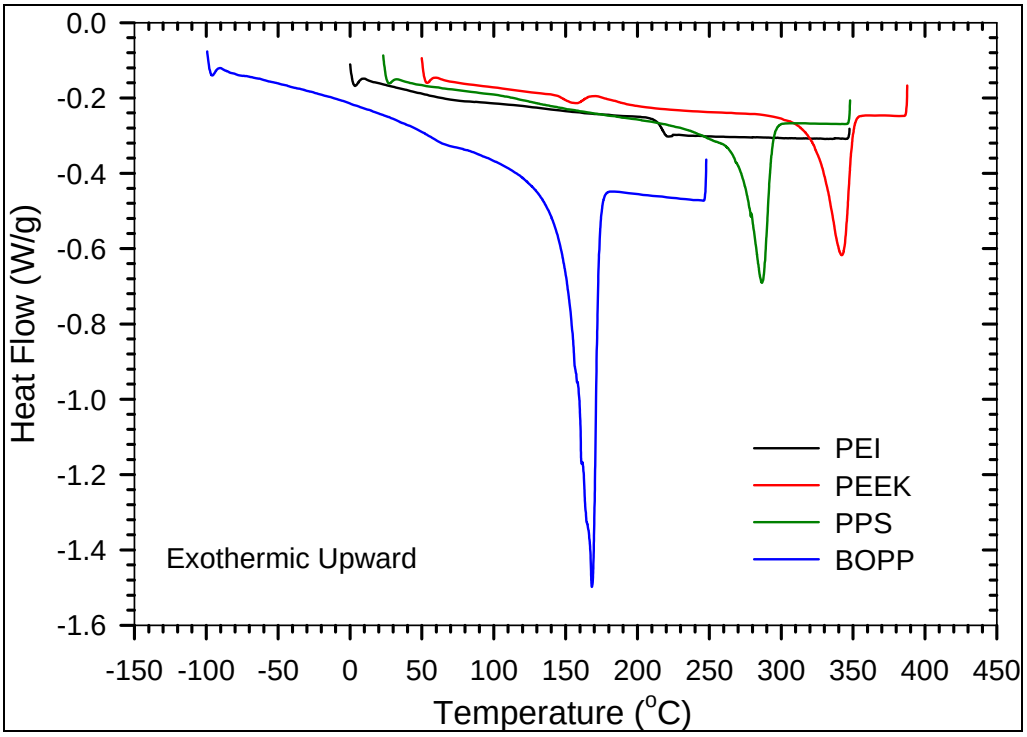

Figure 7. DSC thermograms of the polymers under study at a scan rate of 10 °C/min in nitrogen.

Table 1. Glass transition temperature, crystalline melting temperature, and percent crystallinity of the polymers under study.

Polymer	Glass Transition Temperature (°C)	Melting Temperature (°C)	Heat of Fusion, ΔH_f (J/g)	ΔH_f, 100% Crystallinity (J/g)	Percent Crystallinity
PEI	218	N/A	N/A	N/A	N/A
PEEK	149	342	42.1	130	32.4
PPS	118	287	48.5	112	43.3
BOPP	61	171	100.0	165	61

4.2 Breakdown Strength at Elevated Temperature

The 2-parameter Weibull distribution of breakdown strength for the four polymers at room temperature is shown in figure 8, and the parameters are summarized in table 2. As shown in figure 8, the Weibull characteristic breakdown strength of PEI is about 500 MV/m, which is similar to that of PPS, while PEEK is lower, at around 320 MV/m. The breakdown strength of the high temperature polymers is at least 30% lower than that of BOPP, which is about 700 MV/m. The film quality for PEI appears to be poorer in comparison to the other three polymers, as indicated by wide dispersion of the data.

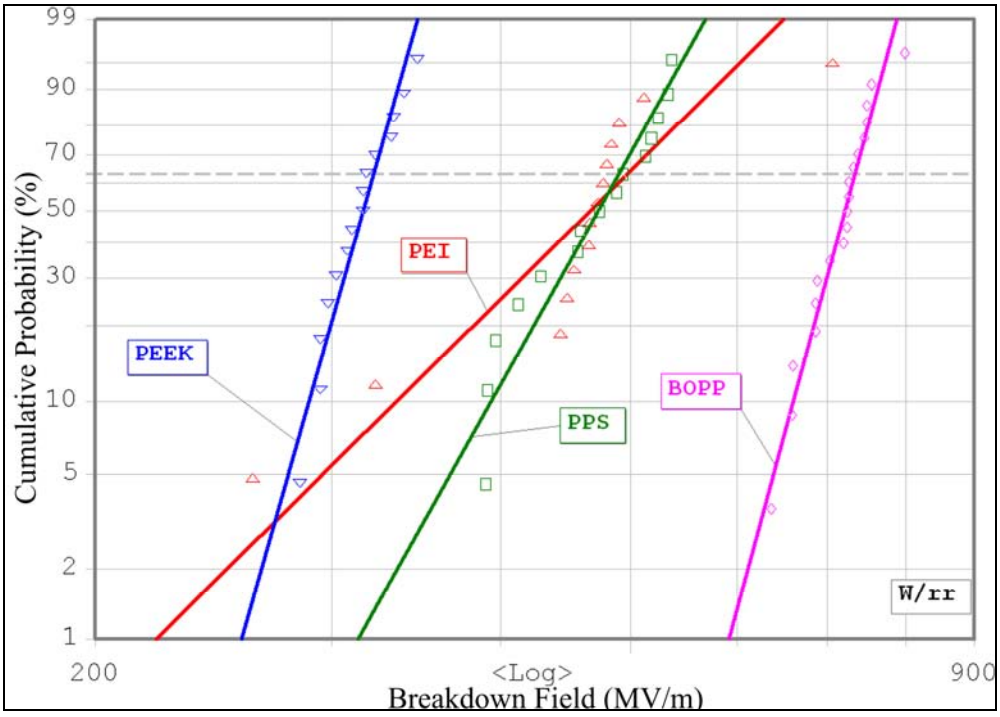

Figure 8. The 2-parameter Weibull distribution of breakdown strength of the polymers under study at room temperature.

Table 2. Summary of the 2-parameter Weibull statistics of the polymers under study at room temperature.

Polymer	Weibull Characteristic Breakdown Field (MV/m)	Slope	Quality of Fit	Number of Samples
PEI	497	5.7	0.813	14
PEEK	322	20.4	0.946	15
PPS	490	10.3	0.929	15
BOPP	733	21.3	0.959	19

Figure 9 shows the Weibull characteristic breakdown strengths with 90% confidence intervals at elevated temperatures for the four polymers. They all show similar behavior, i.e., stable breakdown strength up to some threshold, above which the breakdown strength drops abruptly. For PEEK, PPS, and BOPP, the threshold temperature occurs above their glass transition temperature, while for PEI the threshold is around 150 °C, which is 70 °C below the glass transition temperature. At 150 °C, the decrease in breakdown strength relative to the room temperature value for PEI is about 16% and about 13% for PEEK, while PPS remained unchanged. For BOPP, the maximum test temperature was 100 °C, at which the breakdown strength decreased by about 11% from room temperature.

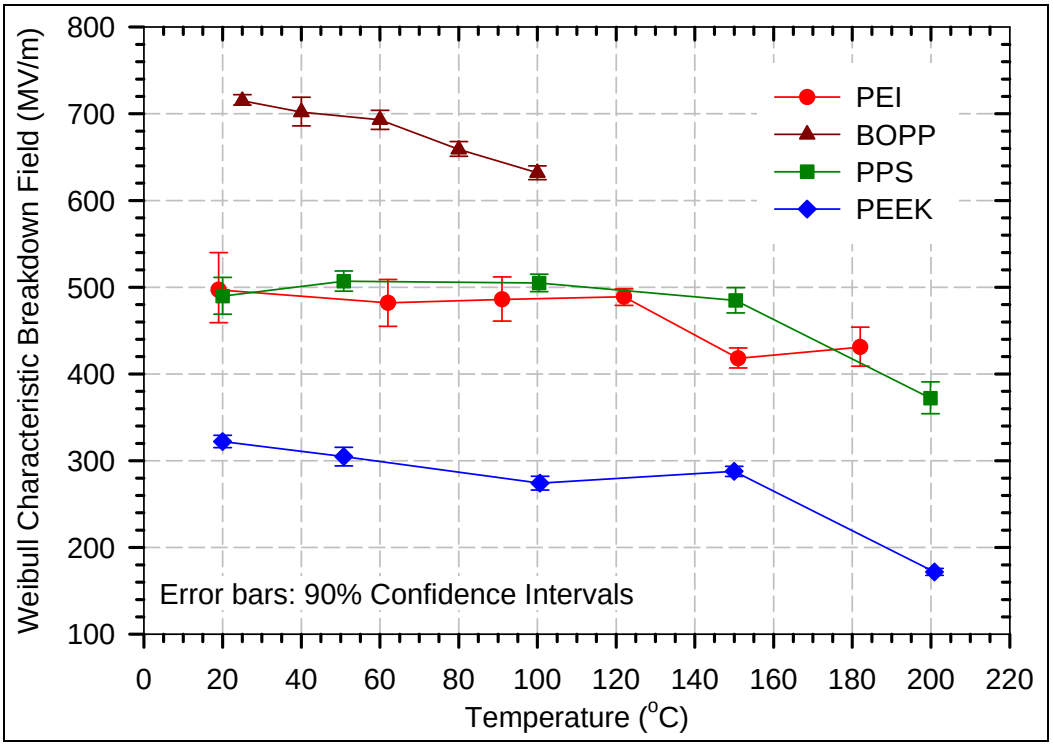

Figure 9. Weibull characteristic breakdown strength as a function of temperature for the polymers under study with 90% confidence limits.

The energy densities of the polymers calculated using breakdown strength at room temperature and at 150 °C are shown in table 3. Although PPS, PEI, and PEEK have dielectric constants about 50% higher than BOPP, their energy densities at room temperature are at least 40% lower than that of BOPP (5 MJ/m^3) due to their significantly lower dielectric strengths, as energy density scales with square of the dielectric strength but only linearly with dielectric constant. The results shown in table 3 suggest that PEI and PEEK do not offer any improvement over PPS, from which capacitors are already available.

Table 3. Energy density of the polymers under study calculated from breakdown strength at temperatures 25 and 150 °C.

Polymer	Dielectric Constant	Breakdown Strength (MV/m), T = 25 °C	Max. Energy Density (MJ/m^3)	Breakdown Strength (MV/m), T = 150 °C	Energy Density (MJ/m^3), T = 150 °C
PEI	3.2	460	3	400	2.3
PEEK	3.1	320	1.4	280	1.1
PPS	3.1	470	3	470	3.0
BOPP	2.25	700	5	NA	NA

4.3 Dielectric Properties at Elevated Temperature

The loss tangent of PEI, PEEK, PPS, and BOPP as a function of frequency at various temperatures are shown in figures 10–12. At 30 °C, the loss tangent of PEI and PEEK is an order of magnitude greater than both of PPS and BOPP, as illustrated in figure 10. As temperature was increased to 95 °C, an increase in dielectric loss with decreasing frequency was apparent, especially in BOPP, as shown in figure 11. As temperature was further increased to above 150 °C (figure 12), similar behavior observed in PEI, PEEK, and PPS became more pronounced. Figure 13 shows the dielectric constant of BOPP at 95 °C and that of the other three polymers at 200 °C along with the data at 30 °C for comparison.

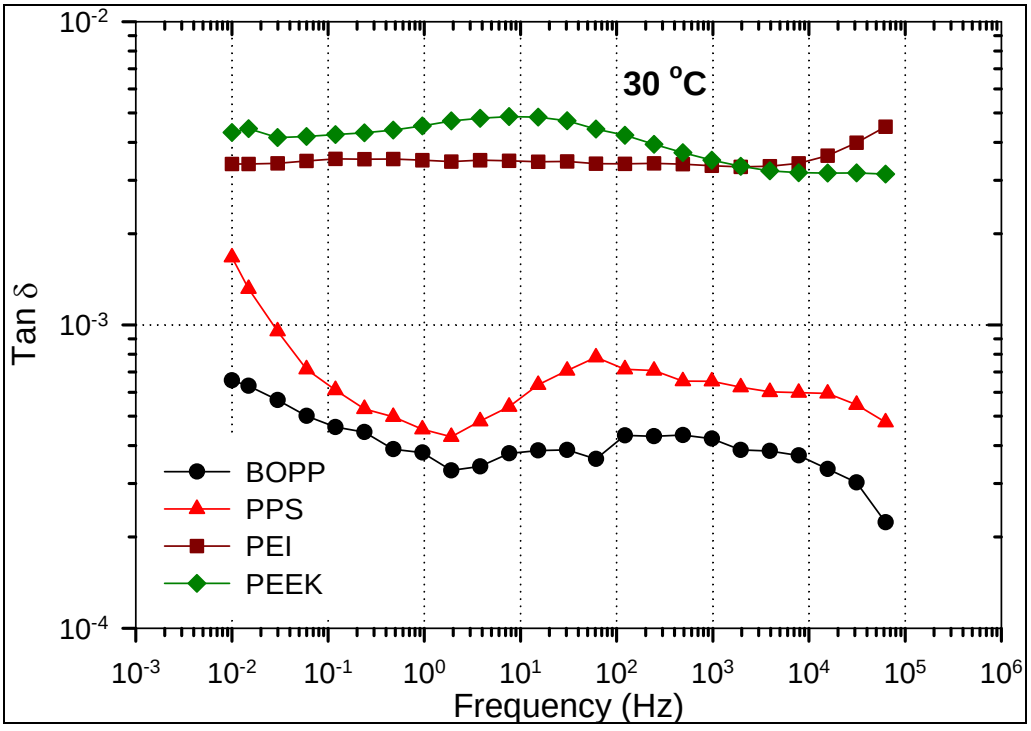

Figure 10. Loss tangent of the polymers under study at room temperature.

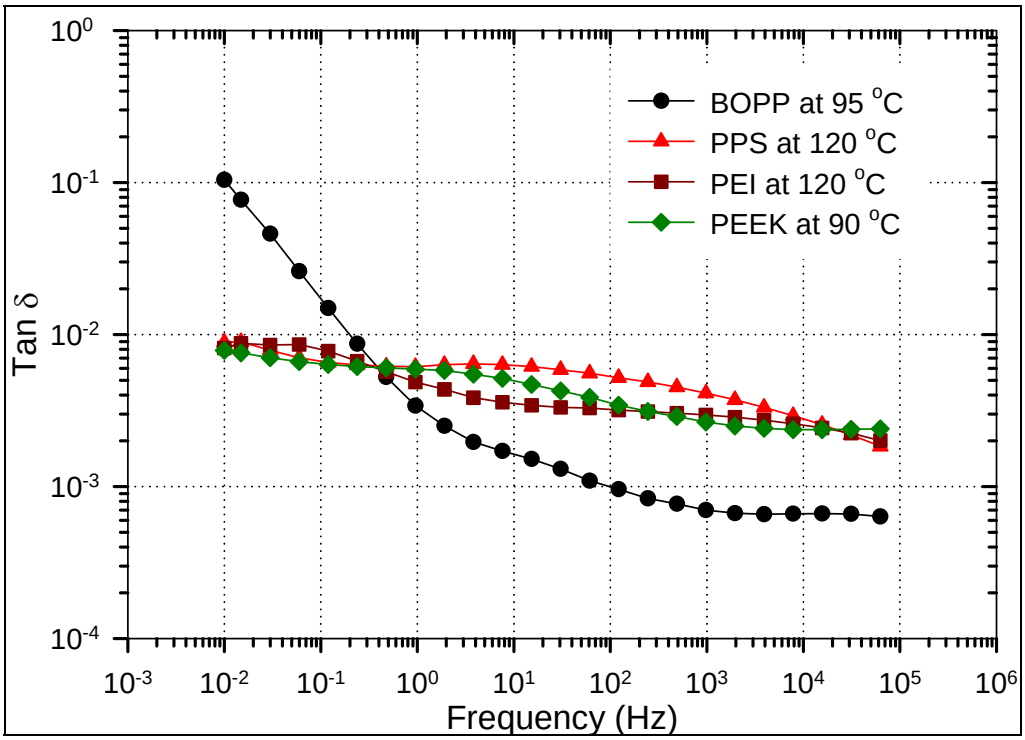

Figure 11. Loss tangent of the polymers under study from 90 to 120 °C.

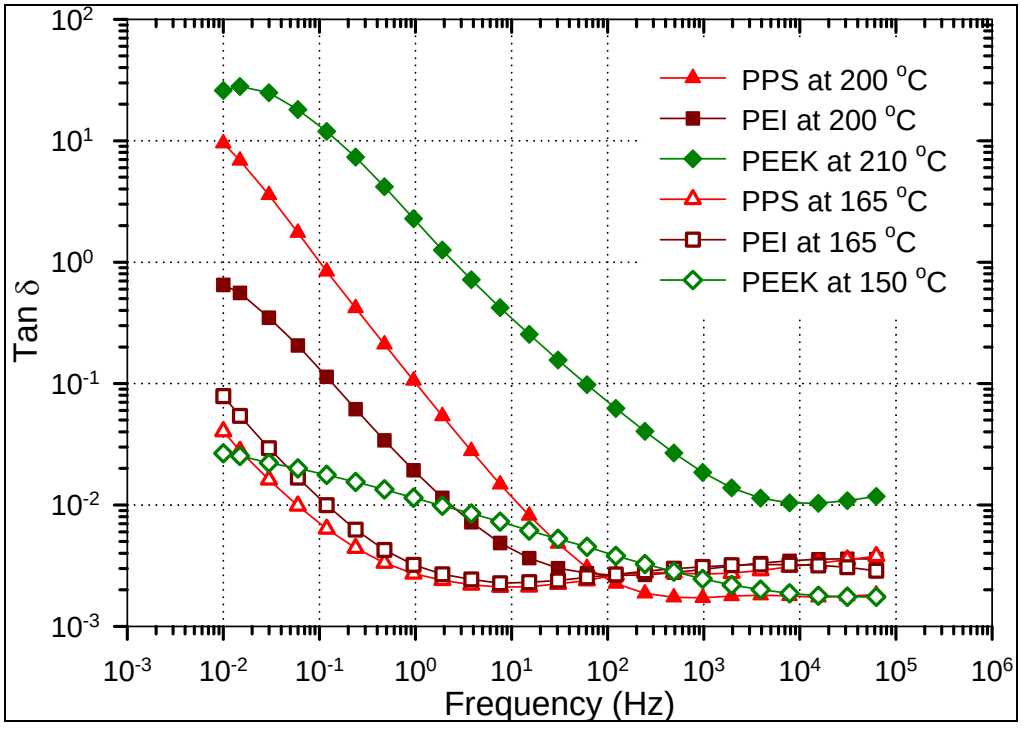

Figure 12. Loss tangent of the polymers under study from 150 to 200 °C.

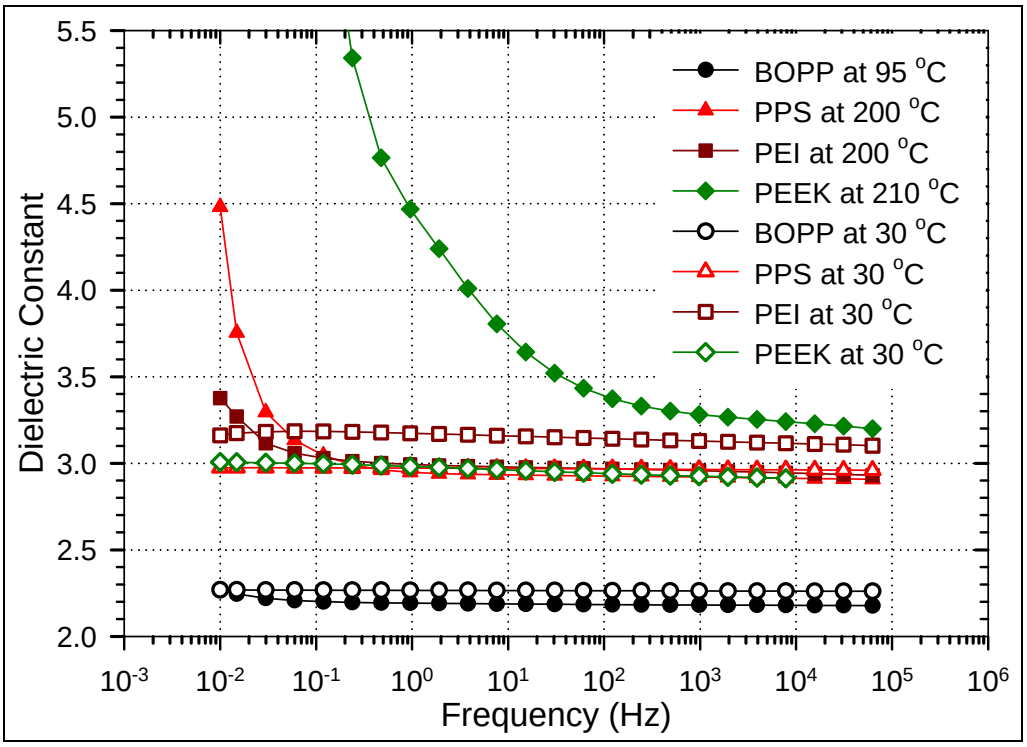

Figure 13. Dielectric constant of the polymers under study at different temperatures.

5. Discussion

The dielectric loss can be decomposed into terms due to relaxation and DC-conductivity, so that the loss tangent can be written as

$$\tan\delta = \frac{\varepsilon''}{\varepsilon'} = \frac{\varepsilon''_{relax} + \varepsilon''_{DC}}{\varepsilon'} = \frac{\varepsilon''_{relax}}{\varepsilon'} + \frac{\sigma}{\varepsilon'\omega}, \qquad (2)$$

where ε' and ε" are the real and the imaginary parts of the dielectric constant, respectively; σ is the DC-conductivity; and ω is the angular frequency. When the loss is dominated by DC-conductivity such that it increases inversely with frequency and therefore exhibits an inverse frequency relationship, the DC-conductivity can be determined using equation 2. As shown in figure 12, loss due to conduction was apparent in PPS at 200 °C but not obvious for BOPP, PEI, or PEEK. Using equation 2, the conductivity for PPS at 200 and 165 °C was calculated as $1.72\text{x}10^{-11}$ S/m and $6.90\text{x}10^{-14}$ S/m, respectively. The room temperature value provided by the manufacturer (*7*) is $2\text{x}10^{-16}$ S/m. Other measurements are required to determine the conductivity for PEI and PEEK. Assuming these two polymers have negligible conductivity, PEI appears to be the better candidate for power electronic applications as the acceptable dissipation factor is below 0.3%. Note that the electrical conductivity obtained above is from low electric field measurements. Under high field at the same temperature, the conductivity will be greater.

5.1 Effect of Electrical Conductivity

Even though a polymer is stable thermally to a high temperature, it may not be used successfully as a high temperature capacitor dielectric. If the electrical conductivity increases too rapidly with temperature, the power dissipation at operating temperature may be sufficient to cause thermal runaway at elevated temperature. The electrical conductivity increases with both temperature and electric field. For good capacitor dielectrics, the change in conductivity with electric field between low field and operating fields is generally quite small. The change in conductivity with temperature generally fits an Arrhenius relationship of the form:

$$\sigma(T) = \sigma_0 \exp(\frac{-Aq}{K_B T}), \tag{3}$$

where σ_0 is A is an activation energy in eV, q is the electronic charge, and K_B is Boltzmann's constant.

5.2 Adiabatic Temperature Rise

The effect of temperature-dependent conductivity can be evaluated in a number of approximations. The simplest approximation is to assume that no heat is lost from the capacitor so that the system is adiabatic, in which case the temperature rise will be the adiabatic temperature rise of the polymer given by the power density (σE^2) times the volumetric heat capacity. This first order evaluation of stability is useful, for if the adiabatic temperature rise is very large, the system must certainly be unstable thermally, while if it is extremely small, the system will be stable.

Figure 14 shows the power density (*PD*) as a function of electric field using the DC-conductivity at 165 and 200 °C calculated for PPS. From the power density, one can calculate the rate of adiabatic temperature rise, (ΔT_{ad}), which is given by

$$\Delta T_{ad} = \frac{PD}{C_v}, \tag{4}$$

where C_v is the volumetric heat capacity. For PPS, a value for C_v of 2.3×10^6 J/(m^3-K) was obtained from the ratio of molar heat capacity (*8*) to the molar volume (*9*), which was assumed to be unchanged at elevated temperature based on the 1.5% increase in density observed from 25 to 270 °C (*5*). Figure 15 shows the rate of adiabatic temperature rise as a function of field.

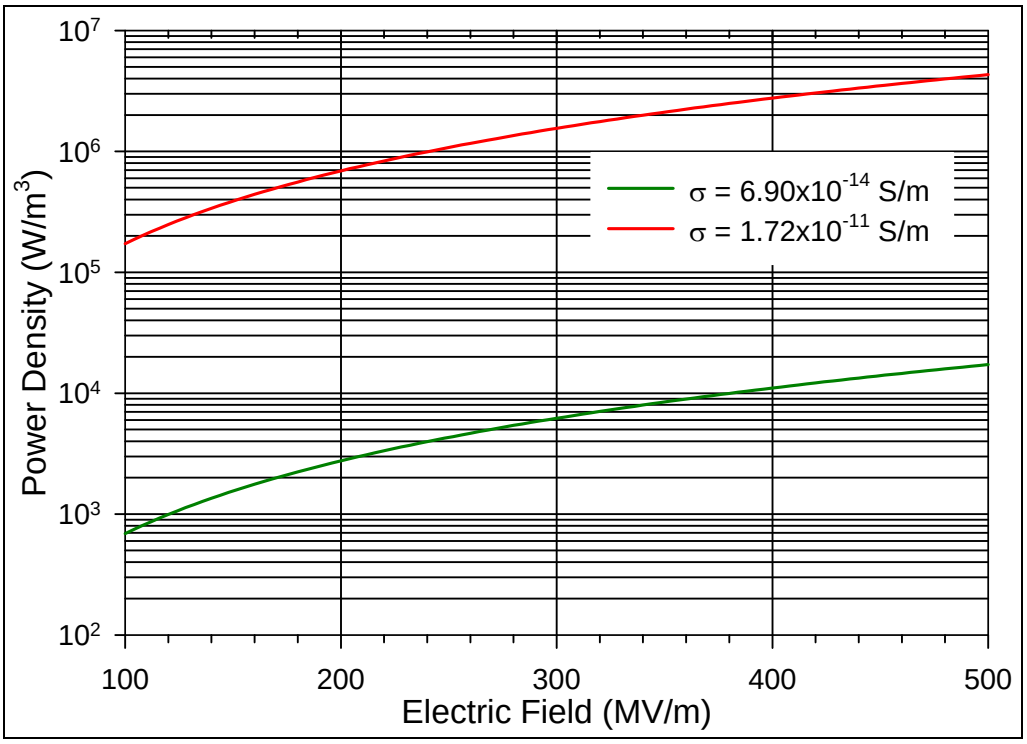

Figure 14. Power density as a function of electric field calculated based on electrical conductivities calculated for PPS at 165 and 200 °C.

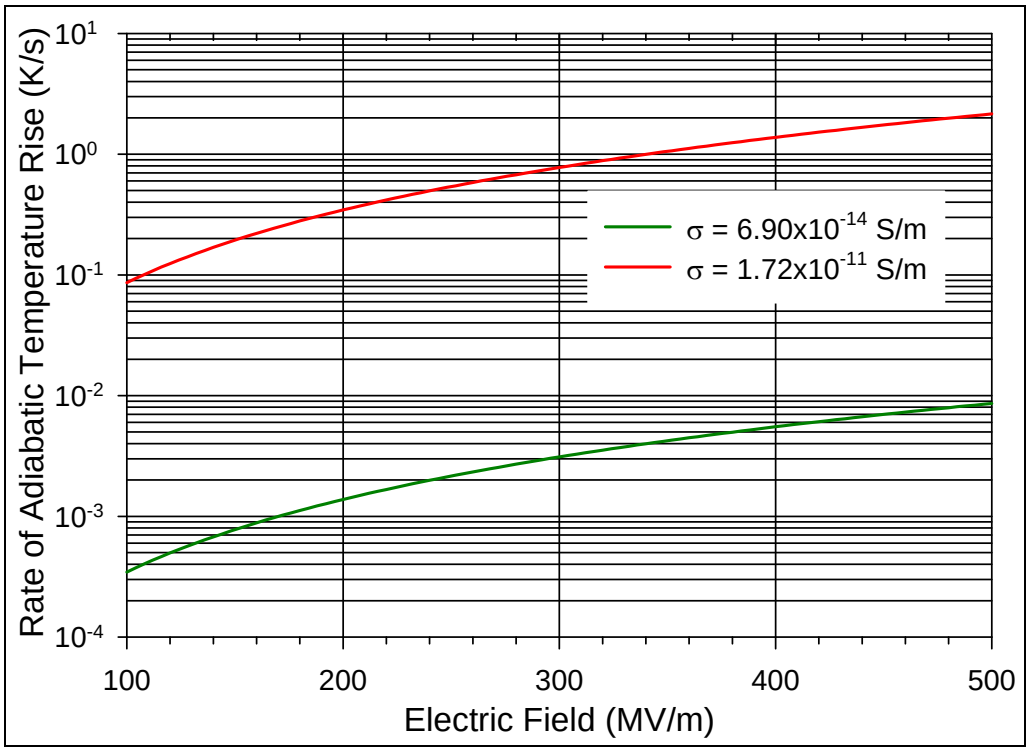

Figure 15. Rate of adiabatic temperature rise as a function of electric field calculated based on electrical conductivities calculated for PPS at 165 and 200 °C.

As shown in figure 15, for a moderate field of 200 MV/m, the rate of adiabatic temperature rise is 1.5×10^{-3} K/s for a conductivity of 6.90×10^{-14} S/m at 165 °C and 0.35 K/s for a conductivity of 1.72×10^{-11} S/m at 200 °C. Given that the capacitors may be at voltage for prolong period of time in certain applications, 0.35 K/s may be excessive but would be too low to have a noticeable effect during breakdown strength measurement.

5.3 Surface Temperature at Constant Power Dissipation

The next level of approximation is to assume an operating field and an initial operating temperature with a corresponding electrical conductivity for the polymer within the capacitor, which results in a uniform power density, as previously described. However, we now assume convective and radiative heat loss from the surfaces of the capacitor enclosure, from which we can compute the enclosure surface temperature. If this surface temperature is comparable to the assumed capacitor dielectric temperature within the enclosure, then the capacitor will probably be unstable. This is because the temperature at the center of the enclosure will be much greater than the enclosure temperature as a result of the poor thermal conductivity of the capacitor dielectric (~0.3 W/m-K), resulting in greater conductivity and power dissipation. As the power dissipated goes as the enclosure volume but the heat loss is determined by the enclosure area, the size of the enclosure has an impact on thermal stability, which decreases with enclosure size, i.e., a large capacitor will be less stable than a small capacitor.

By assuming a solid rectangular geometry, a capacitor enclosure surface temperature, T_{cs}, at steady state can be obtained by solving the heat balance equation given as

$$PD \cdot V = h \cdot A \cdot (T_{cs} - T_{am}) + \sigma_{SB} \cdot \varepsilon \cdot A \cdot (T_{cs}^4 - T_{am}^4), \tag{5}$$

where PD is the power density generated due to electrical conductivity; V and A are the volume and surface area of the capacitor, respectively; h is the convective heat transfer coefficient of 20 W/(m^2-K); T_{am} is the ambient temperature; σ_{SB} is the Stefan-Boltzmann constant; and ε is the emissivity of the enclosure surface, which is 1 for an ideal black body and <1 for others. For the present calculation $\varepsilon = 1$ is used. Table 4 summarizes the data for three capacitor sizes for the two electrical conductivities assuming an operating electric field of 200 MV/m at an ambient temperature of 27 °C. As shown in table 4, PPS, which has a low-field electrical conductivity of 6.90×10^{-14} S/m at 165 °C, should be useable at this temperature, as indicated by the negligible temperature rise. However, at 200 °C with a conductivity of 1.72×10^{-11} S/m, the temperature is unstable.

Table 4. Capacitor surface temperature at steady state for various rectangular sizes at E-field of 200 MV/m and 27 °C ambient temperature.

Capacitor Size (cm^3)	**T_{cs} (°C) at Steady State**	
	$\sigma = 6.90 \times 10^{-14}$ S/m	**$\sigma = 1.72 \times 10^{-11}$ S/m**
3 x 3 x 10	28	168
10 x 10 x 5	28	257
60 x 30 x 45	34	622

5.4 Temperature Distribution Based on Constant Rate of Heat Generation

For uniformly distributed power dissipation within the capacitor with convective heat loss from the enclosure, the temperature distribution within the capacitor can be computed both as a function of time as the capacitor comes to thermal equilibrium (transient case) and for final the equilibrium temperature distribution. The steady state solutions for the case of an infinite rectangular solid can be found in Carslaw and Jaeger (*10*, p. 171), as can the transient solution for the temperature distribution within an infinite solid bounded by two planes (*10*, p. 133), i.e., the case ignoring heat loss from the edges, top and bottom. As the electrical conductivity and therefore, the power dissipation of the dielectric is a strong function of temperature, these solutions are probably not much more useful than the two simpler approximations presented previously.

5.5 Temperature Distribution from Transient Nonlinear Finite Element Analysis

The most accurate approach to computing thermal stability is a three-dimensional (3D) transient nonlinear finite element thermal computation with fixed applied voltage, temperature-dependent electrical conductivity, and convective/radiative boundary conditions, employed as discussed earlier. Using modern multiphysics programs (e.g., COMSOL), such computations are relatively simple, as long as the temperature-dependent conductivity is known. If the capacitor dielectric conductivity is known as a function of temperature and electric field, such a computation can be undertaken with coupled electric and thermal fields. In such computations, the temperature distribution is computed as a function of time, and thermal runaway is indicated by divergence of the temperature in some region of the capacitor dielectric.

As noted previously, thermal stability for given dielectric properties is a function of ambient temperature, enclosure size and shape, and boundary conditions. For example the convective heat transfer coefficient in still air is typically about 20 W/m^2-K, but for air motion in the range of 1 m/s, this can increase by an order of magnitude. Thus thermal stability will be sensitive to the conditions of use. The thermal conductivity of metallized polymer film is anisotropic as a result of the metallization. Although the metallization thickness is only about 0.1% of the film thickness, the metallization thermal conductivity is about 1000 times greater than that of the polymer. Thus thermal conduction in the plane of the film should be substantially greater than that through the film, although no data are presently available. Measurements are underway to quantify this effect. As multiphysics programs allow the thermal conductivity to be anisotropic, such effects could be included in 3D transient nonlinear finite element models used to evaluate thermal stability.

6. Conclusions

In summary, the breakdown strength measurements and dielectric properties at elevated temperatures for PEEK and PEI were compared to those for PPS and BOPP, which represent the present state of the art. The breakdown strength at room temperature for PEEK was the lowest at about 320 MV/m, while strength for both PPS and PEI was 500 MV/m and for BOPP was 720 MV/m. At 150 °C, the decrease in breakdown strength relative to room temperature for PEI is about 16% and about 13% for PEEK, while PPS remained unchanged. For BOPP, the maximum test temperature was 100 °C, at which the breakdown strength decreased by about 11%. Based on the results of breakdown strength measurements, PEEK and PEI appear to offer no improvement over PPS, from which capacitors are already available. However, results from dielectric loss measurements seem to indicate that PPS has a greater electrical conductivity at 200 °C than PEEK or PEI. Moreover, PEI has a lower loss than PEEK at temperatures above 150 °C and frequencies higher than 1 kHz. Therefore, PEI appears to be the better candidate for power conditioning capacitors. More measurements are needed to determine the conductivity of PEEK and PEI.

7. References

1. Reed, C. W.; Cichanowski, S. W. The Fundamentals of Aging in HV Polymer-film Capacitors. *IEEE Transactions on Dielectrics and Electrical Insulation* **1994**, *1* (5), 904–922.
2. Dissado, L. A.; Fothergill, J. C. *Electrical Degradation and Breakdown in Polymers*; Peter Peregrinus Ltd., London, Ch. 14, 1992.
3. Abernethy, R. B. *The New Weibull Handbook*, 3rd ed.; R. B. Abernethy, Palm Beach, FL, Ch. 2, 1998.
4. Zoller, P.; et al. The Equation of State and Heat of Fusion of Polyetheretherketone. *Journal of Polymer Science Part B: Polymer Physics* **1989**, *27*, 993–1007.
5. Huo, P.; Cebe, P. Effect of Thermal History on the Rigid Amorphous Phase in Poly(phenylene sulfide). *Colloid and Polymer Science* **1992**, *270*, 840–852.
6. Gaur, U.; Wunderlich, B. Heat Capacity and Other Thermodynamic Properties of Linear Macromolecules. IV. Polypropylene. *Journal of Physical and Chemical Reference Data* **1981**, 1051–1064.
7. Torelina® PPS Film Technical Information, Toray, Japan, May 1999.
8. Cheng, S. Z. D.; et al. Glass Transition and Melting Behavior of Poly(thio-1,4-phenylene. *Macromolecules* **1987**, *20*, 2802–2810.
9. Brandrup, J. et al. *Polymer Handbook*, 4th ed.; Wiley-Interscience: New York, Chapter VII, 1999, pp. 675–714, Molar volume obtained by using Group Contribution Methods by Fedors.
10. Jaeger, J.C.; Carslaw, H.S. *Conduction of Heat in Solids*, 2nd Ed.; Oxford Science Publications, Oxford, 1986.

List of Symbols, Abbreviations, and Acronyms

3D	three-dimensional
BOPP	biaxially oriented polypropylene
DSC	differential scanning calorimetry
PC	polycarbonate
PEEK	poly(ether ether ketone)
PEI	poly(ether imide)
PEN	poly(ethylene napthalate)
PET	poly(ethylene terephthalate)
PPS	poly(phenylene sulfide)
RC	resistor capacitor
SCR	silicon controlled rectifier
SiC	silicon carbide

NO. OF COPIES	ORGANIZATION
1 ELEC	ADMNSTR DEFNS TECHL INFO CTR ATTN DTIC OCP 8725 JOHN J KINGMAN RD STE 0944 FT BELVOIR VA 22060-6218
1	DARPA ATTN IXO S WELBY 3701 N FAIRFAX DR ARLINGTON VA 22203-1714
1 CD	OFC OF THE SECY OF DEFNS ATTN ODDRE (R&AT) THE PENTAGON WASHINGTON DC 20301-3080
1	US ARMY RSRCH DEV AND ENGRG CMND ARMAMENT RSRCH DEV AND ENGRG CTR ARMAMENT ENGRG AND TECHNLGY CTR ATTN AMSRD AAR AEF T J MATTS BLDG 305 ABERDEEN PROVING GROUND MD 21005-5001
1	PM TIMS, PROFILER (MMS-P) AN/TMQ-52 ATTN B GRIFFIES BUILDING 563 FT MONMOUTH NJ 07703
1	US ARMY INFO SYS ENGRG CMND ATTN AMSEL IE TD A RIVERA FT HUACHUCA AZ 85613-5300
1	COMMANDER US ARMY RDECOM ATTN AMSRD AMR W C MCCORKLE 5400 FOWLER RD REDSTONE ARSENAL AL 35898-5000
1	US GOVERNMENT PRINT OFF DEPOSITORY RECEIVING SECTION ATTN MAIL STOP IDAD J TATE 732 NORTH CAPITOL ST NW WASHINGTON DC 20402

NO. OF COPIES	ORGANIZATION
1	US ARMY RSRCH LAB ATTN RDRL CIM G T LANDFRIED BLDG 4600 ABERDEEN PROVING GROUND MD 21005-5066
5	US ARMY RSRCH LAB ATTN IMNE ALC HRR MAIL & RECORDS MGMT ATTN RDRL CIM L TECHL LIB ATTN RDRL CIM P TECHL PUB ATTN RDRL SED C J HO ATTN RDRL SED C R JOW ADELPHI MD 20783-1197

TOTAL: 14 (1 ELEC, 1 CD, 12 HC)